RSC Advances

PAPER

View Article Online
View Journal | View Issue

Cite this: *RSC Adv.*, 2017, **7**, 12161

Solvent-dependent and highly selective anion sensing and molecular logic application of bisindolylmaleimide derivatives†

Huimei Yao,[a] Jingwei Wang,[a] Huan Chen,[b] Xiaofei Mei,[b] Zhu Su,[a] Jingnan Wu,[a] Zhenghuan Lin*[a] and Qidan Ling*[ab]

Received 18th December 2016
Accepted 15th February 2017

DOI: 10.1039/c6ra28367e

rsc.li/rsc-advances

A series of bisindolylmaleimide dyes (IMs) with different *N*-substituents (IM-PFB, IM-TBA and IM-MB) and planarity (IMC-MB and IM-MB) were designed and synthesized to detect anions selectively and sensitively. The anion-sensing properties were investigated systematically by changing the *N*-substituents of maleimide, solvent type and molecular planarity. Results indicate that the anion recognition is significantly affected by the solvent type rather than the *N*-substituents. Different anion sensitivity in various solvents makes IMs selectively detect F^- in ACN, $H_2PO_4^-$ in DCM and CN^- in THF. Due to the fixed location of two NH groups, the dye IMC-MB with planar structure exhibits poor sensing selectivity in various solvents. The titration curves of anions show that the sensing mechanism of IMs in various solvents for anions is different. The further experimental and DFT/TDDFT calculation results demonstrate that the hydrogen bond interaction and deprotonation of one H atom take place in DCM and THF, respectively, and that the two interactions synchronously exist in ACN. Interestingly, the solvent-dependent anion recognition can make IM-PFB mimic the function of three kinds of decoders (1-to-2, 2-to-3 and 2-to-4), a 4-to-2 encoder and a 1 : 2 demultiplexer. It is really rare for one molecule to mimic so many logic operations.

Introduction

To develop an effective detection method for anions has become an important subject due to the crucial role of anions in biological, chemical and environmental systems, especially in the fields of biological metabolites, food additives, drugs, agricultural fertilizers, and waste liquids.[1–3] Among anions, cyanide, fluoride and phosphate can cause huge damage to the environment, such as the production of toxic waste, water contamination and eutrophication, and nerve gases.[4–6] Consequently, there is demand for sensitive, selective and easy-to-manipulate methods for detecting these three kinds of toxic anions. However, compared to the cation binding and sensing, anion detection is more challenging for their large size, variable shape, weak electrostatic interactions, and strong solvation effects.[7] In addition, various non-covalent interactions, such as hydrogen bonding, hydrophobicity, and coordination to metal center, would impose a huge effect on the recognition of anions.[8,9] As a kind of simple detection method of anions, fluorimetric probing and sensing have attracted wide interest of researchers for excellent sensitivity, good specificity, a large linear range of analysis, and ease of handling.[10] The interactions of anions with fluorescent sensors often introduce new optical transitions or excited states and lead to changes in the photophysical properties (such as the absorption spectra, emission intensity, or lifetime, *etc.*), which can then act as an indicator of anion recognition.[11,12]

Molecular logic gates are an interdisciplinary research area that could make integrated circuits smaller and more efficient, compared with traditional silicon-based circuits.[13,14] As a result, mimicking digital logic operations of the real world in the molecular level has attracted increasing interest.[15] Since the first AND molecular logic gate was reported by De Silva,[16] all kinds of molecular systems mimicking the functions of logic devices, even complicated computing operation (such as multiplexer, demultiplexer, adder, subtractor, encoder and decoder *etc.*), have been developed in the last two decades.[13,17–19] Stimuli-responsive fluorescent materials display great potential in the field of molecular computing for their excellent sensitivity, good specificity, a large linear range of analysis, and ease of handling.[17,20–22] If the conversation process from external stimuli (cation/anion, acid/base, redox, DNA, light, heat, chemicals and electricity) to the response in the photophysical properties complies with the binary Boolean logic rules, the function of logic devices can be

[a]*College of Materials Science and Engineering, Fujian Key Laboratory of Polymer Materials, Fujian Normal University, Fuzhou 350007, China*

[b]*College of Chemistry and Chemical Engineering, Fujian Normal University, Fuzhou 350007, China. E-mail: zhlin@fjnu.edu.cn; lingqd@fjnu.edu.cn*

† Electronic supplementary information (ESI) available: Absorption and emission spectra, photophysical and TD-DFT calculation data, titration curves, as well as Job's plot. See DOI: 10.1039/c6ra28367e

realized by employing the stimulus and response as input and output, individually.[23–29]

Anion recognition of fluorescent sensors is frequently used to construct the molecular logic system for the significant availability of anion interaction.[25,26,30–32] However, one sensor molecule always responds to anions in one channel, which means that selective detecting multiple anions need different sensors, and that complex molecular design, incorporating other functional groups into the sensor, is necessary to meet the need of logic operation.[33,34] If one molecule can selectively sense multiple anions (such as F^-, CN^- and $H_2PO_4^-$ *etc.*) in different signaling channels, it is desirable for both selective anion recognition and molecular logic computing.

Indolylmaleimide derivatives have been successfully applied in organic light-emitting diode as electroluminescent materials, due to their strong luminescence in both solid and solution.[35–38] Recently, we expand the application of the 3,4-diarylmaleimide derivatives with N–H functional groups (indole, pyrrole or amide) to sense anions.[39,40] Maleimide, as an electron-deficient group, can help enhance the acidity and H-bond binding ability of N–H group in the indole rings. As a result, the optical properties of indolylmaleimides are sensitive to NH-anion interactions, thus suitable for both colorimetric and fluorimetric detections of anions. It is necessary to investigate systematically the effect of different *N*-substituent of maleimide, solvents and molecular planarity on the sensing capacity of indolylmaleimides to obtain one compound sensing multiple anions in different ways. To this end, in this paper, a series of 3,4-bisindolylmaleimide dyes (IMs, Scheme 1) with N–H groups were designed and synthesized to detect anions in different solvents. It is found that medium polarity and molecular planarity have an important influence on the selectivity of anions recognition. Through changing the solvent from ACN, DCM to THF, IM-PFB could selectively detect F^-, CN^- and $H_2PO_4^-$. According to the results, three kinds of decoders (1-to-2, 2-to-3 and 2-to-4), a 4-to-2 encoder and a 1 : 2 demultiplexer have been constructed by IM-PFB.

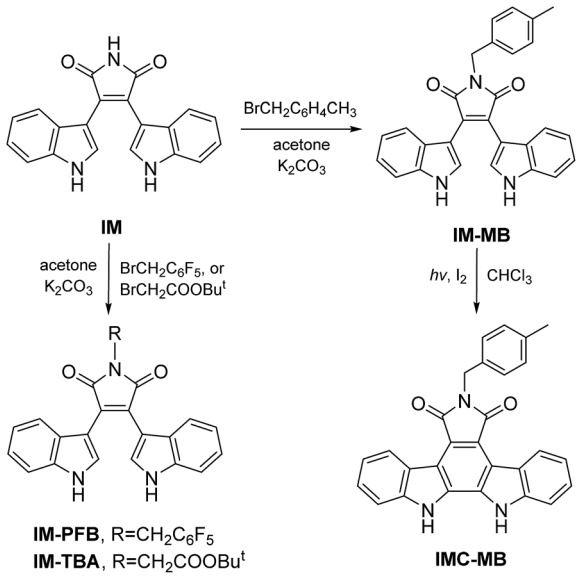

Scheme 1 Structure and synthesis of bisindolylmaleimide derivatives.

Experimental section

General

Electronic spray ion (ESI) mass spectra were recorded on a Bruker micrOTOF II spectrometer. NMR spectra were measured in $CDCl_3$, *d*-acetone or *d*-DMSO on a Bruker Ascend 400 FT-NMR spectrometer; ^1H and ^{13}C chemical shifts were quoted relative to the internal standard tetramethylsilane. UV-vis spectra were obtained on a Shimadzu UV-2600 spectrophotometer. The PL spectra were probed on a Shimadzu RF-5301PC fluorescence spectrophotometer. All photographs were recorded on a Canon Powershot G7 digital camera under daylight or UV light (365 nm) lamp. The fluorescence quantum yields were determined in CH_3CN solutions at 293 K against Nile red as a reference ($\Phi_p = 0.78$).[41]

All of the reagents and solvents used were obtained from commercial suppliers and were used without further purification unless otherwise noted. Thin layer chromatography was performed on G254 plates of Qingdao Haiyang Chemical. Column chromatography was performed on Sorbent Technologies brand silica gel (40–63 mm, Standard grade).

Synthetic procedure of IM-PFB, IM-TBA and IM-MB

To a solution of IM (1.5 g, 4.6 mmol) in acetone (12 mL) under a nitrogen atmosphere were added bromide (4.6 mmol) and K_2CO_3 (0.76 g, 5.5 mmol). The mixture was allowed to be stirred for 12 h at ambient temperature. The mixture was successively extracted with ethyl acetate and washed with water and brine. It was then dehydrated over anhydrous $MgSO_4$. After removing the solvent, the crude product was purified by column chromatography with ethyl acetate/petroleum ether (1 : 5) as the eluant, affording pure dark red solids in 41–77% yield.

Physical data for IM-PFB (68%). ^1H NMR ($CDCl_3$, 400 MHz): δ 8.58 (s, 2H), 7.75 (d, 2H), 7.32 (d, 2H), 7.07 (t, 2H), 6.94 (d, 2H), 6.75 (t, 2H), 4.97 (s, 2H). ^{13}C NMR (*d*-DMSO, 100 MHz): δ 171.03, 146.69, 144.18, 138.54, 136.46, 129.87, 127.33, 125.72, 122.16, 121.41, 119.88, 112.26, 111.00, 105.96, 30.02. HRMS (ESI) *m*/*z* $[M]^+$ calcd 507.1006, found 507.1000.

Physical data for IM-TBA (41%). ^1H NMR (*d*-acetone, 400 MHz): δ 10.80 (s, 2H), 7.83 (d, 2H), 7.47 (d, 2H), 6.97 (t, 2H), 6.93 (d, 2H), 6.62–6.66 (m, 2H), 4.30 (s, 2H), 1.40 (s, 9H). ^{13}C NMR (*d*-acetone, 100 MHz): δ 171.27, 166.92, 136.43, 129.67, 127.65, 125.88, 121.93, 121.44, 120.00, 111.07, 106.50, 81.43, 39.91, 27.26. HRMS (ESI) *m*/*z* $[M]^+$ calcd 441.1689, found 441.1683.

Physical data for IM-MB (77%). ^1H NMR ($CDCl_3$, 400 MHz): δ 8.47 (s, 2H), 7.76 (d, 2H), 7.38–7.31 (m, 4H), 7.06–7.15 (m, 4H), 6.95 (d, 2H), 6.74 (t, 2H), 4.81 (s, 2H), 2.31 (s, 3H). ^{13}C NMR (*d*-DMSO, 100 MHz): δ 171.92, 137.01, 136.45, 134.78, 129.80, 129.60, 128.00, 127.34, 125.81, 122.14, 121.40, 119.86, 112.25, 106.05, 41.33, 21.13. HRMS (ESI) *m*/*z* $[M]^+$ calcd 431.1634, found 431.1628.

Synthetic procedure of compound IMC-MB

To a red solution of IM-MB (0.67 g, 1.56 mmol) in 500 mL of benzene was added iodine (0.04 g (0.156 mmol)). The reaction

mixture continuously bubbled with air was irradiated with a medium pressure mercury lamp for 8 h. The crude products were diluted with ethyl acetate, extracted with saturated $Na_2S_2O_4$, rinsed with brine, dried over Na_2SO_4, filtered, and concentrated in vacuum. Purification by flash chromatography with ethyl acetate/petroleum ether (1 : 4) as the eluant yielded 0.8366 g (57%) of IMC-MB as a yellow solid.

Physical data for IMC-MB (57%). ^{1}H NMR ($CDCl_3$, 400 MHz): δ 9.31 (s, 2H), 9.04 (d, 2H), 7.51–7.37 (m, 8H), 7.15 (d, 2H), 4.87 (s, 2H), 2.30 (s, 3H). ^{13}C NMR (*d*-DMSO, 100 MHz): δ 169.99, 140.84, 136.92, 135.04, 130.09, 129.55, 128.00, 127.39, 124.66, 121.90, 120.76, 119.01, 116.21, 112.56, 40.90, 21.11. HRMS (ESI) m/z $[M]^+$ calcd 429.1477, found 429.1471.

Evaluation of sensing capability

The evaluation of anion-sensing capability of IM-PFB, IM-TBA, IM-MB and IMC-MB was performed in acetonitrile (ACN), dichloromethane (DCM) and tetrahydrofuran (THF) by the addition of the tetrabutylammonium salt of various anions such as NO_3^-, Br^-, HSO_4^-, Cl^-, OAc^-, CN^-, $H_2PO_4^-$, F^- and I^-. These solvents are analytic reagent and used without drying. All of evaluation experiments including optical spectra collecting were performed under air atmosphere. Freshly prepared samples in 1 cm quartz cells were used for all absorption and emission measurements.

Results and discussion

Synthesis and photophysical properties

The synthetic route of four bisindolylmaleimide dyes (IMs) was presented in Scheme 1. IM-PFB, IM-TBA and IM-MB were obtained readily from 3,4-bis(3-indolyl)-maleimide[42] through an alkylation under alkaline condition. IM-MB went through an oxidative cyclization catalyzed by I_2 and UV light to give IMC-MB. All of the resulting compounds were characterized by ^{1}HNMR, ^{13}CNMR and high resolution mass spectra.

In THF solution, IM-PFB, IM-TBA and IM-MB exhibit similar absorption and emission properties with their normalized spectra shown in Fig. 1. It indicates that the spectral properties of these compounds in solution are not influenced much by changing the *N*-substituent on maleimide. There are three major absorption bands in the range of 250–550 nm regions of their UV-vis spectra. The band before 320 nm is assigned to a π–π^* transition localized mainly on the indole group.[43] The low energy bands after 320 nm are derived from the transitions involving both indole and maleimide units, because neither of them alone exhibits an absorption band after 325 nm. The broad featureless band at about 457 nm displays an intramolecular charge-transfer (ICT) character, which corresponds to an electron transition from indole to maleimide.[44] Charge recombination from the excited state gives a red emission at 597–602 nm showing an apparent solvent shift (Fig. S1†), with 30–34% of the quantum efficiency (Table S1†).

Compared to IM-PFB, IM-TBA and IM-MB, IMC-MB shows a completely different absorption and emission spectra in solution, due to its flat structure (Fig. 1). There are two major

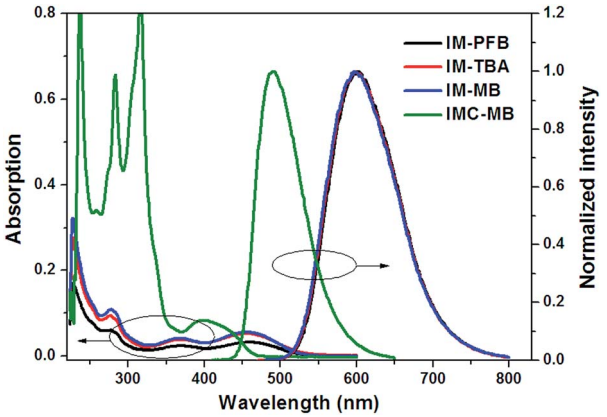

Fig. 1 Absorption and normalized emission spectra of sensors in THF (50 μM).

absorption bands in the absorption spectrum of IMC-BM after 260 nm, one in the UV region around 317 nm, with shoulder at 283 nm, and the other one around 399 nm in the visible region, which can be assigned to π–π^* transitions from the S_0 to the S_2 and S_1 states, respectively. When irradiated at 399 nm, IMC-MB exhibits intense green luminescent at 490 nm with a higher quantum yield of 39% as compared to IM-MB (Table S1†).

Qualitative evaluation

Effect of substituent. The qualitative evaluation of anion sensing capability of IM-MB, IM-TBA and IM-PFB was performed in acetonitrile by the addition of the tetrabutylammonium salt of various anions such as NO_3^-, Br^-, HSO_4^-, Cl^-, OAc^-, CN^-, $H_2PO_4^-$, F^- and I^- (Fig. 2, S2 and S3†). As noted in Fig. 2a, IM-MB exhibits highly selective sensing for F^- with fluorescence quenching and color change from yellow to purple. The color change of IM-MB upon F^- is originated from the disappearance of the absorption band around 455 nm along with two new peaks at 565 nm and 323 nm (Fig. 2b). The ratio of absorption intensities at 565 nm and 455 nm (I_{565}/I_{455}) presents a 265 fold enhancement, from 0.02 without F^- to 5.3 with F^- (20 eq.). When IM-TBA and IM-PFB was added by F^-, similar alteration in absorption spectra was found. The ratio of I_{565}/I_{455} increases 1876 fold for IM-TBA and 2671 fold for IM-MB with F^- (100 eq.), as shown in Fig. S2a and S3b.† In addition, the peak around 606 nm in the emission spectra almost disappears after the addition of F^- (Fig. 2c, S2b and S3c†). Consequently, IM-PFB, IM-TBA and IM-MB, as a kind of colorimetric and fluorescent sensors, can efficiently and selectively detect fluoride in ACN solution. The above results also indicate that *N*-substituents of maleimide are insignificant for their selective recognition of anions.

Effect of solvent. As mentioned before, the 3,4-bisindolylmaleimide dyes are of ICT character, resulting in their emission affected by the polarity of solvents. Would the polarity of solvents impose effect on their sensing for anions? To answer this question, the qualitative evaluation of anion recognition of these 3,4-bisindolylmaleimides IMs was further proceeded in DCM and THF solvents. In DCM (Fig. 3a, c and S4†), IM-TBA

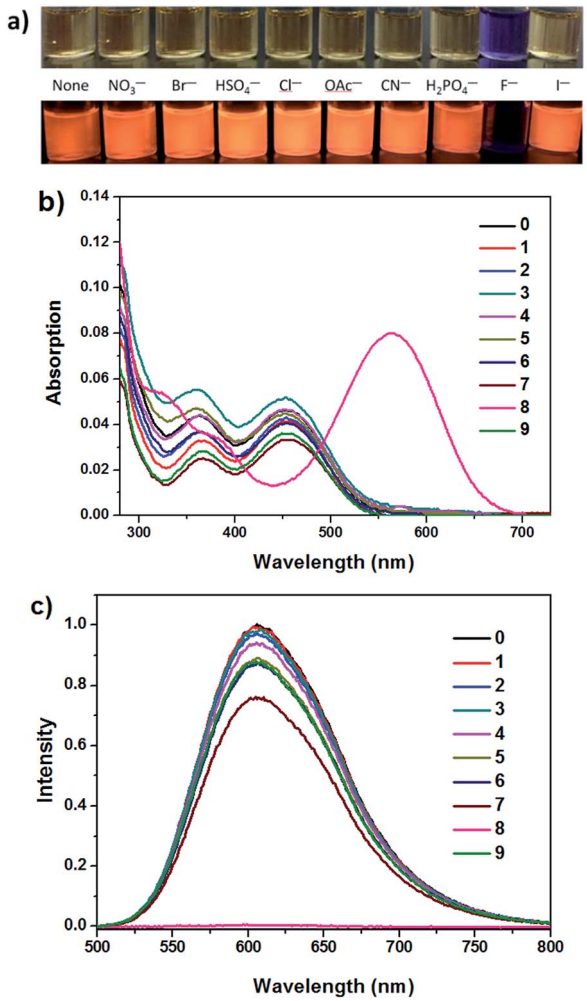

Fig. 2 (a) Photograph of IM-MB (50 μM in ACN) in the presence of various anions (20 eq.) under daylight (top) and UV light (bottom). Absorption (b) and emission (c) spectra of IM-MB (50 μM in ACN) in the presence of anions (20 eq.). Anions arrangement: 0-none, 1-NO_3^-, 2-Br^-, 3-HSO_4^-, 4-Cl^-, 5-OAc^-, 6-CN^-, 7-$H_2PO_4^-$, 8-F^-, 9-I^-.

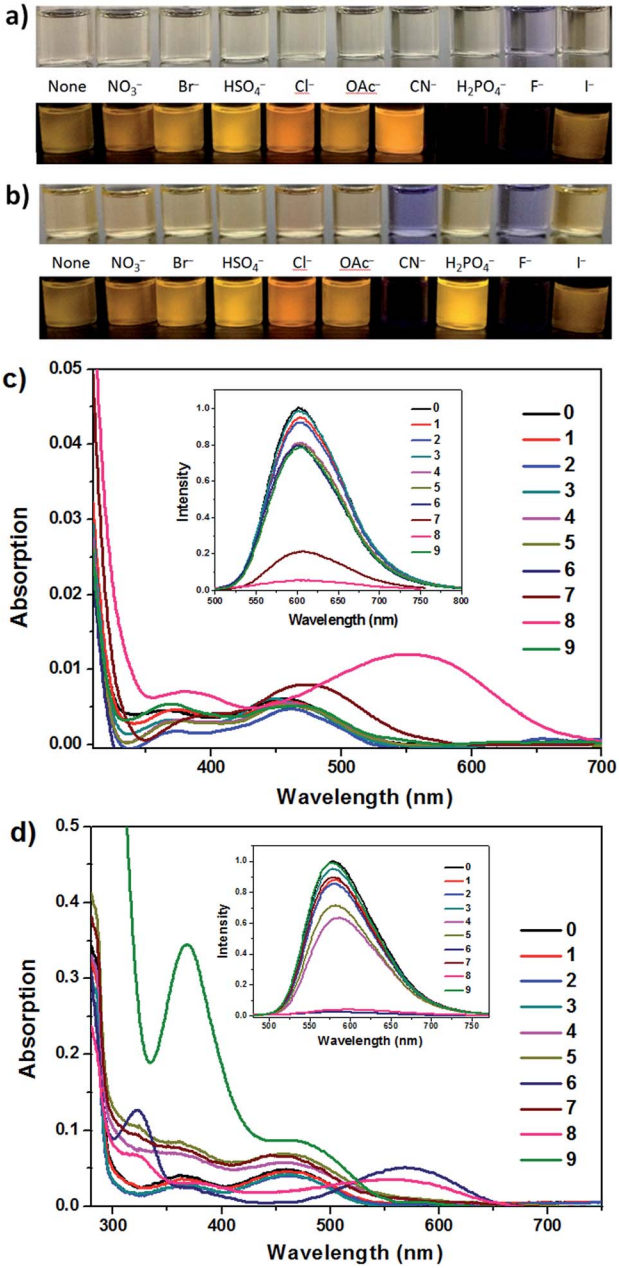

Fig. 3 Photograph of IM-TBA (50 μM) in DCM (a) and THF (b) upon various anions (100 eq.) under daylight (top) and UV light (bottom). Absorption and emission (inset) spectra of IM-TBA (50 μM) in DCM (c) and THF (d) upon anions (100 eq.). Anions arrangement: 0-none, 1-NO_3^-, 2-Br^-, 3-HSO_4^-, 4-Cl^-, 5-OAc^-, 6-CN^-, 7-$H_2PO_4^-$, 8-F^-, 9-I^-.

and IM-PFB show similar sensing ability as the previous reported bisindolylmaleimide.[40] That is, only F^- induces the color of IM-TBA and IM-PFB change from faint yellow into lavender. However, both $H_2PO_4^-$ and F^- cause their fluorescent quenching in DCM. Differently from the change of absorption spectra of IM-PFB and IM-TBA upon F^- in ACN, their absorption bands around 370 nm and 460 nm show a bathochromic shift in DCM upon the addition of 100 eq. of $H_2PO_4^-$ and F^-. For example, the maximum absorption wavelength of IM-TBA shifts from 456 nm to 473 nm upon $H_2PO_4^-$ and to 551 nm upon F^- (Fig. 3c). The emission intensity of IM-TBA in DCM at 604 nm is quenched 86% and 94% by $H_2PO_4^-$ and F^-, respectively (Fig. 3c inset).

In THF (Fig. 3b, d and S5†), obvious response to the optical properties of IM-TBA and IM-PFB is found after addition of CN^- and F^-. Their change in absorption and emission spectra is similar as that induced by F^- in ACN. For instance, the absorption band of IM-TBA around 460 nm in THF disappears, accompanied by two new peaks at 570 nm and 323 nm in the presence of CN^- (Fig. 3d). Although the degree of fluorescent quenching of IM-TBA and IM-PFB by CN^- and F^- is considerable, their colorimetric sensing sensitivity (I_{570}/I_{460}) for CN^- is much bigger than that for F^-.

Effect of cyclization. IMC-MB obtained by the cyclization of IM-MB was employed to investigate the effect of the planarity of 3,4-bisindolylmaleimide on sensing for anions (Fig. S6–S8†). As mentioned above, IM-MB showed an effectively colorimetric and fluorescent recognition only for F^- in ACN. However, the difference of absorption spectra of IMC-BM in the presence of

various anions is inconspicuous in ACN (Fig. S6b†). There are four kinds of anions (OAc^-, CN^-, $H_2PO_4^-$ and F^-) causing an impressive decline in emission intensity of IMC-BM (Fig. S6c†). In DCM and THF solvent, IMC-BM also exhibited poorer selectivity of anion sensing than IM-PFB and IM-TBA (Fig. S7 and S8†), which should be attributed to its weak ICT character and acidity of NH in indole units, as well as the fixed location of two NH receptor for anion recognition. Thus, the relative orientation between the two NH groups of IMs should be important in selective sensing for anions.

Selective recognition of anions. It can be found that the solvent environment of these dyes play a more important role in the selective recognition of anions than substituent and molecular planarity. They showed different spectra response to anions in different solvents. Taking IM-TBA for example, based on above the qualitative evaluation (Fig. S2,† 3c and d), the intensity changes of its absorption and emission spectra in different solvents are summarized in Fig. 4. If the ordinate value of absorption (Fig. 4a, c and e) more than 3 or emission (Fig. 4b, d and f) less than 0.5, are considered response to anions, the response of IM-TBA to anions in different solvents can be summarized in Table 1. In THF solvent, the response on both the absorption and emission of IM-TBA is caused by CN^-, while only response to its emission induced by F^-. In DCM solvent, response to emission, not to absorption of IM-TBA was found in the presence of $H_2PO_4^-$. Only F^- can lead to both of absorption and emission response of IM-TBA in ACN and DCM solvents. Consequently, IM-TBA can selectively recognize CN^- in THF, and $H_2PO_4^-$ in DCM, and F^- in ACN through monitoring its optical performance of the absorption and emission.

Table 1 Response of IM-TBA to anions in different solvents[a]

	ACN		DCM		THF[a]	
	uv	pl	uv	pl	uv	Pl
CN^-	—	—	—	—	R	R
$H_2PO_4^-$	—	—	—	R	—	—
F^-	R	R	R	R	—	R
Others	—	—	—	—	—	—

[a] R represents response to anion.

Spectra titration in different solvent

The titration curves of fluoride for IM-PFB and IM-MB in ACN are similar and shown in Fig. 5a, b and S9,† respectively. Their absorption peaks at 455 nm and 367 nm decrease upon addition of fluoride along with the increasing of 564 nm and 325 nm bands. Two distinct isosbestic points can be found at 493 and 343 nm, indicating the formation of a stable new species. In their emission spectra in ACN, the intensity of 609 nm band decreases gradually with the increase in the concentration of F^-, accompanied by a small red-shift of the maximum wavelength. When the amount of F^- reaches 10 eq., the emission peaks shifted to 641 nm almost disappears in ACN.

The spectra response of IM-PFB to F^- and $H_2PO_4^-$ in DCM differs from that in ACN (Fig. 5c, d and S10†). Taking F^- for example, the long wavelength absorption at 462 gradually and bathochromically shifts to 520 nm with the amount of F^- increasing from 0 to 60 eq. Concurrently, the emission intensity at 604 nm decreases to 3% without apparent wavelength shift. When the amount of F^- further increased to 80 eq., the absorption and emission spectra keep untouched. The change is similar as that of the reported bisindolylmaleimide titrated by anions in DCM, which indicate IM-PFB should sense F^- and $H_2PO_4^-$ through hydrogen bonding interaction.[40]

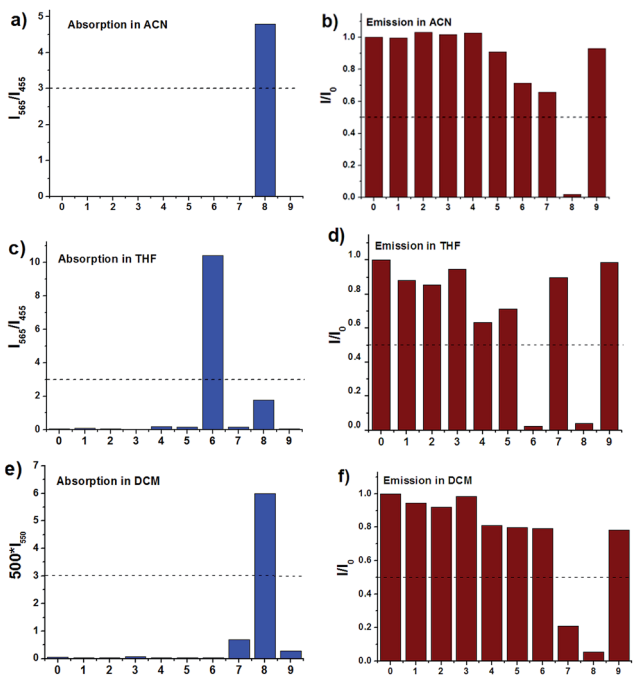

Fig. 4 The ratio of absorption intensity I_{565}/I_{455} (a and c) of IM-TBA in ACN and THF upon various anions (100 eq.). The absorption intensity at 550 nm (e) of IM-TBA in DCM upon various anions (100 eq.). The relative emission intensity (b, d and f) of IM-TBA at 609 nm in the presence of anions (100 eq.). Anions arrangement: 0-none, 1-NO_3^-, 2-Br^-, 3-HSO_4^-, 4-Cl^-, 5-OAc^-, 6-CN^-, 7-$H_2PO_4^-$, 8-F^-, 9-I^-.

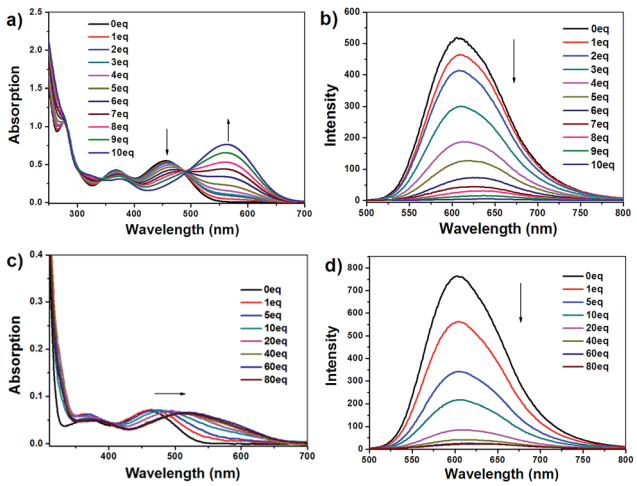

Fig. 5 Absorption (a and c) and emission (b and d) spectra of IM-PFB (5 μM) in ACN (a and b) and DCM (c and d) upon titration of F^-.

In THF solvent, IM-PFB can selectively detect CN^- and F^- from other anions with the titration curves displayed in Fig. S11 and S12.† Upon titration of CN^- and F^- in THF, the absorption spectra of IM-PFB exhibit similar change trend as that of titration of F^- in ACN. That is, absorption band at 466 nm reduces with concomitant growth of two new bands at 575 nm and 321 nm. However, the quenching degree of emission in THF is less than that in ACN. For instance, 10 eq. of F^- can quench the fluorescence of IM-PFB and IM-MB in ACN to 9% and 1%, respectively. While 10 eq. of F^- and CN^- can only cause the emission intensity of IM-PFB in THF decrease to 44% and 14%, respectively.

Sensing mechanism

IM-PFB was chosen as a model to analyze the sensing mechanism of anions. As mentioned above, IM-PFB should sense F^- and $H_2PO_4^-$ in DCM through hydrogen bonding interaction because there is no distinct isosbestic points found in the titration absorption spectra.[40] The titration spectra of anions in ACN and THF indicate that IM-PFB possibly detects F^- and CN^- in a different way for the formation of new species. There are mainly two kinds of sensing mechanism of sensors based on the NH group as recognition sites: hydrogen bonding and deprotonation.[40,45,46] Consequently, it can be supposed that IM-PFB in ACN and THF could be turned into anion by F^- or CN^- through a deprotonation reaction. To verify the supposition, the reactions of IM-PFB with a strong base $N(Et)_4OH$ in different solvents, as well as theory calculations were employed to analyze the optical properties of IM-PFB and its anion. Fig. S13† shows the absorption and fluorescence spectra of IM-PFB (50 μM) in DCM upon the addition of different amounts of $N(Et)_4OH$. With the increasing concentration of OH^-, the absorption peak at 457 nm gradually disappears, accompanied with the appearance of a new absorption peak at around 570 nm and the reduction of emission intensity. Similar situation was found in solvents THF and ACN with the new absorption peak appeared at 576 nm and 566 nm, individually (Fig. S14 and S15†). In ACN, with the continued increase of OH^- amount, another new absorption peak at 648 nm replaces the peak at 566 nm. The first new peak at about 570 nm and the second new peak at around 650 nm should be assigned to monovalent and divalent anion of IM-PFB (IM-PFB$^-$ and IMPFB^{2-}), corresponding to the deprotonation of one hydrogen atom and two hydrogen atoms, individually. It would be confirmed by the following results of theory calculation.

Molecular optimization and optical transitions of IM-PFB and its anions were performed by the density function (DFT) and time-dependent density function (TD-DFT) theory with B3LYP using 6-31G(d) basis sets. In the optimized geometry of IM-PFB (Fig. 6b), the two indole rings are oriented anti to each other, with two N atoms pointing outward. Its electron density distributions of HOMO and LUMO can be depicted in Fig. 6a. As expected the electron density in the HOMO of IM-PFB is mainly populated on two symmetrically equivalent indolyl moieties, while the LUMO is localized on the central maleimide moiety. A charge separation is expected to be produced when

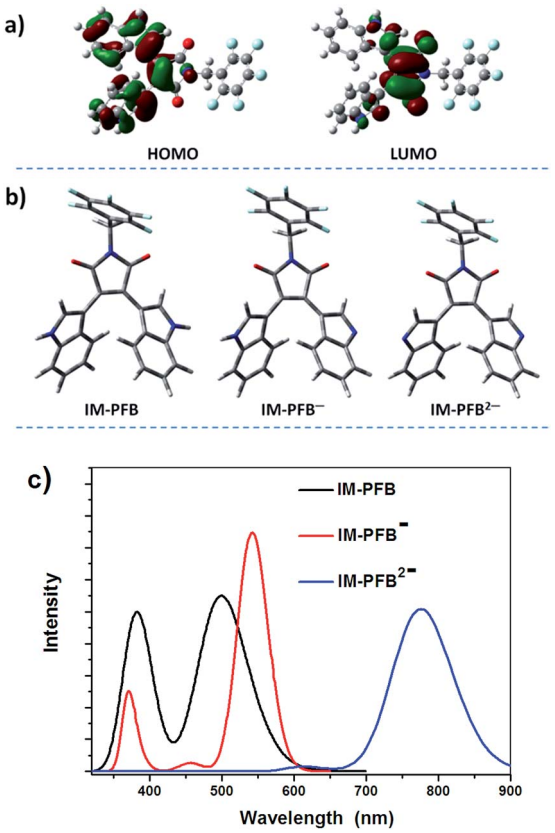

Fig. 6 Electron density distributions of HOMO and LUMO of IM-PFB (a). Optimized geometry (b) and stimulated absorption spectra (c) of IM-PFB and its anion.

an electron is promoted from the HOMO to the LUMO, which make the NH group of indole rings easy to form a hydrogen bond or be deprotonated by a base. From the optimized structure of IM-PFB$^-$ and IMPFB^{2-} (Fig. 6b), deprotonation does not change much the geometries of indole rings. The absorption spectra of IM-PFB and its anions were simulated by TD-DFT calculations and showed in Fig. 6c with the calculated data summarized in Table S2.† The wavelength correlates remarkably well with the experimental results of IM-PFB treated with OH^- (Fig. S13–S15†). For example, the calculated main absorption wavelengths of IM-PFB, IM-PFB$^-$ and IMPFB^{2-} are 499 nm, 544 nm and 775 nm with oscillator strengths of 0.14, 0.19 and 0.13, respectively. As a results, the new absorption of IM-PFB in ACN and THF at around 570 nm induced by F^- or CN^- should be ascribed to deprotonation of one H atom, not two H atoms.

Solvent polarity affects greatly the sensing ways of IM-PFB with anions. The possible interaction mechanism of IM-PFB with anions is outlined in Scheme 2. IM-PFB can form two adducts III and IV through hydrogen bond with one anion and two anions, respectively. III and IV would undergo a deprotonation to produce I and II in polar solvents. The binding stoichiometry of IM-PFB with F^-, $H_2PO_4^-$ and CN^- in various solvents was determined by Job's plots (Fig. S16†). Job's plot of IM-PFB shows the 1 : 2 binding stoichiometry in ACN and DCM, and the 1 : 1 binding stoichiometry in THF with anions.

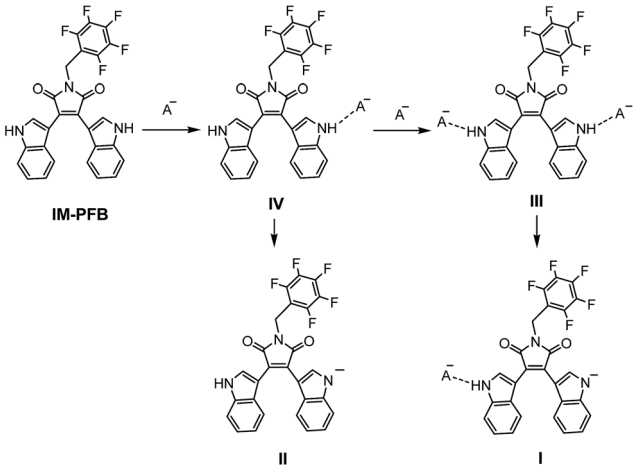

Scheme 2 Possible interaction mechanism of IM-PFB with anions (A^-) in different solvents.

Based on the results, three interaction forms of IM-PFB with anions in different solvents are expected: (I in ACN; II in THF; III in DCM).

Molecular logic operations

The different interaction ways of IM-PFB with anions in different solvents arouse our interests in its applications in molecular logic system. Based on the distinct response to anions, IM-PFB molecules can be employed to construct various logic devices. First, the changes of peak intensity at 607 nm in emission ($I_{E,607}$) and 570 nm in absorption ($I_{A,570}$) in ACN (Fig. S17, ESI†) are utilized as two outputs (O1 and O2) to design a 1-to-2 decoder and a 1 : 2 demultiplexer (Fig. S18†). If fluoride (50 eq.) is taken as only one input (In), the absence and presence of F^- would cause the opposite results in $I_{E,607}$ (O2 = 1 and 0) and $I_{A,570}$ (O1 = 0 and 1) of IM-PFB. As a result, a 1-to-2 decoder was obtained (Fig. S18a†). If IM-PFB and F^- are defined as two inputs (In1 and In2), the function of 1 : 2 demultiplexer can be realized (Fig. S18b†). When In2 (or address input) is set off, O1 ($I_{E,607}$) reports the state of In1 (IM-PFB) and O2 ($I_{A,570}$) remains off, whereas when In2 is switched on, O2 replaces O1 to report the state of In1 and O1 turns off.

Secondly, as shown in Fig. S19 and S20 (ESI†), IM-PFB in DCM can function as a 2-to-3 decoder by employing the stimuli of F^- and $H_2PO_4^-$ as two inputs (In1 and In2), and the response of the emission intensity at 604 nm ($I_{E,604}$), the absorption intensity at 560 nm ($I_{A,560}$), and the ratio of absorption intensity at 467 nm and 350 nm ($I_{A,467/350}$) as three outputs (O1, O2 and O3). When no input was applied (In1 = In2 = 0), IM-PFB exhibits strong orange emission (O1 = 1), no obvious absorption band at 560 nm (O2 = 0) and comparable absorption at 467 nm and 350 nm (O3 = 0). After In1 or In2 was applied, O1 ($I_{E,604}$) was turned off for the fluorescence of IM-PFB in DCM quenched by F^- or $H_2PO_4^-$, but O2 ($I_{A,560}$) or O3 ($I_{A,467/350}$) was turned on for the change of absorption spectra in 560 nm or 350 nm.

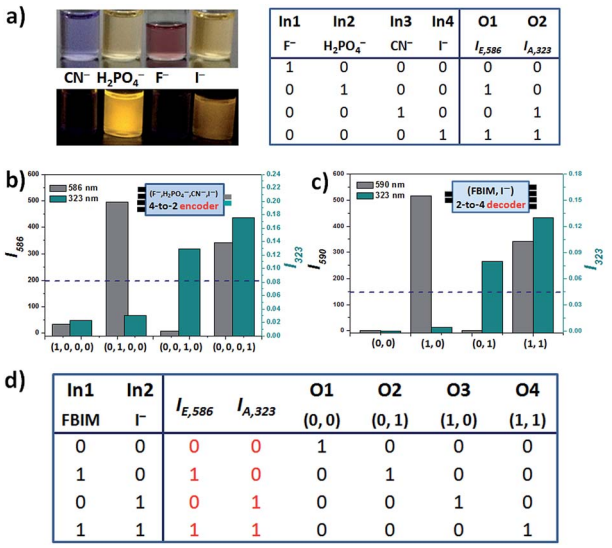

In1 F^-	In2 $H_2PO_4^-$	In3 CN^-	In4 I^-	O1 $I_{E,586}$	O2 $I_{A,323}$
1	0	0	0	0	0
0	1	0	0	1	0
0	0	1	0	0	1
0	0	0	1	1	1

In1 FBIM	In2 I^-	$I_{E,586}$	$I_{A,323}$	O1 (0, 0)	O2 (0, 1)	O3 (1, 0)	O4 (1, 1)
0	0	0	0	1	0	0	0
1	0	1	0	0	1	0	0
0	1	0	1	0	0	1	0
1	1	1	1	0	0	0	1

Fig. 7 4-to-2 encoder (a and b) and 2-to-4 decoder (c and d) demonstrated by the response of the emission intensity at 586 nm ($I_{E,586}$) and the absorption intensity at 323 nm ($I_{A,323}$) to F^-, $H_2PO_4^-$, CN^- and I^- in THF.

Last, IM-PFB in THF can mimic the logic operation of two reversible data-processing devices: 4-to-2 encoder and 2-to-4 decoder. When utilizing IM-PFB as a 4-to-2 encoder, the inputs are defined as 50 eq. of F^- (In1), $H_2PO_4^-$ (In2), CN^- (In3) and I^- (In4). The intensity of the fluorescence at 586 nm ($I_{E,586}$) and the absorptions at 323 nm ($I_{A,323}$) are considered as O1 and O2, respectively. As shown in Fig. S21 (ESI†), the emission at 586 nm of IM-PFB can be significantly quenched by F^- and CN^-, not by I^- and $H_2PO_4^-$. This means that both In1 and In3 can turn O1 off, while In2 and In4 make O1 on. On the other hand, it is CN^- and I^-, not F^- and $H_2PO_4^-$ that can induce a strong absorbance at 323 nm. It means that O2 can be switched on by In3 and In4. Thus, the truth table of the 4-to-2 encoder is represented as shown in Fig. 7. In addition, IM-PFB can be also easily reconfigured to behave as a molecular 2-to-4 encoder, when IM-PFB and I^- act as two inputs (Fig. 7d). If $I_{E,586}$ and $I_{A,323}$ are also selected as two outputs, it was found that there are four different output results: (0, 0), (0, 1), (1, 0) and (1, 1). If taking the four output results as four kinds of new outputs (O1, O2, O3 and O4), the decoder function of IM-PFB can be demonstrated.

Conclusions

Bisindolylmaleimide derivatives (IMs) based on amine group as receptor were synthesized and found sensitive to anions with obvious colorimetric effect and fluorescence quenching. IM-PFB, IM-TBA and IM-MB with two twisted indole rings exhibit better selectivity for anions than IMC-MB with planar aromatic rings, due to their flexible recognition sites of NH groups. Interestingly, anion sensing of IM-PFB, IM-TBA and IM-MB behaves strong dependence on solvent types. For example, in ACN, F^- can make IM-PFB form a new absorption

peak at 564 nm and quench its emission at 609 nm. In DCM, $H_2PO_4^-$ causes significant fluorescence quench of IM-PFB and little impact on its absorption. In THF, CN^- can induce the large response to both the absorption and emission of IM-PFB like F^- in ACN. OH^- experiment and theory calculation indicate that the new absorption peak at around 570 nm is the result of deprotonation of one H atom. Based on the Job plots analysis, three possible interaction forms of IM-PFB with anions in different solvents are presented. Based on the anion-sensing behavior of IM-PFB, three decoders (1-to-2, 2-to-3 and 2-to-4), a 4-to-2 encoder and a 1 : 2 demultiplexer have been developed. These results indicate IMs are good candidates for mimicking molecular logic computing.

Acknowledgements

This work was supported by the National Natural Science Foundation of China (21374017, 21401023 and 21574021), Specialized Research Fund for the Doctoral Program of Higher Education (20123503120002), Program for Innovative Research Team in Science and Technology in Fujian Province University (IRTSTFJ), the Natural Science Foundation of Fujian Province (2013H0018), and Educational Commission of Fujian Province (JA12059 and JA14068).

Notes and references

1 J. E. Bailey, M. Bohner, C. J. Brinker, B. Cornils, T. Evans, H. Greim, L. L. Hegedus, J. Heitbaum, W. Keim, A. Kleemann, G. Kreysa, J. Loliger, J. L. McGuire, A. Mitsutani, L. Plass, G. Stephanopoulos, D. Werner, P. Woditsch and N. Yoda, *Ullmann's Encyclopedia of Industrial Chemistry*, Wiley VCH, New York, 6th edn, 1999.
2 A. Bianchi, K. Bowman-James and E. Garcia-Espana, *Supramolecular Chemistry of Anions*, Wiley-VCH, New York, 1997.
3 E. R. Riegel and J. A. Kent, *Riegel's handbook of industrial chemistry*, Springer, 10th edn, 2003.
4 K. W. Kulig and B. Ballantyne, *Cyanide toxicity, US Department of Health & Human Services*, Atlanta, GA, 1991.
5 B. L. True and R. H. Dreisbach, *Dreisbach's handbook of poisoning*, Parthenon Pub. Group, 2002.
6 P. Singh, M. Barjatiya, S. Dhing, R. Bhatnagar, S. Kothari and V. Dhar, *Urol. Res.*, 2001, **29**, 238–244.
7 Y. Marcus, *J. Chem. Soc., Faraday Trans.*, 1991, **87**, 2995–2999.
8 M. H. Keefe, K. D. Benkstein and J. T. Hupp, *Coord. Chem. Rev.*, 2000, **205**, 201–228.
9 A. S. Singh and S.-S. Sun, *Chem. Commun.*, 2011, **47**, 8563–8565.
10 M. S. T. Gonçalves, *Chem. Rev.*, 2009, **109**, 190–212.
11 M. Sun, S. Wang, Q. Yang, X. Fei, Y. Li and Y. Li, *RSC Adv.*, 2014, **4**, 8295–8299.
12 C.-Y. Hung, A. S. Singh, C.-W. Chen, Y.-S. Wen and S.-S. Sun, *Chem. Commun.*, 2009, 1511–1513.
13 J. Andreasson and U. Pischel, *Chem. Soc. Rev.*, 2010, **39**, 174–188.
14 A. P. de Silva and S. Uchiyama, *Nat. Nanotechnol.*, 2007, **2**, 399–410.
15 F. Pu, J. Ren and X. Qu, *Adv. Mater.*, 2014, **26**, 5742–5757.
16 P. A. de Silva, N. H. Q. Gunaratne and C. P. McCoy, *Nature*, 1993, **364**, 42–44.
17 D. Margulies, G. Melman and A. Shanzer, *Nat. Mater.*, 2005, **4**, 768–771.
18 D. Margulies, G. Melman and A. Shanzer, *J. Am. Chem. Soc.*, 2006, **128**, 4865–4871.
19 J. Andreasson, U. Pischel, S. D. Straight, T. A. Moore, A. L. Moore and D. Gust, *J. Am. Chem. Soc.*, 2011, **133**, 11641–11648.
20 M. S. T. Gonçalves, *Chem. Rev.*, 2009, **109**, 190–212.
21 X. Mei, G. Wen, J. Wang, H. Yao, Y. Zhao, Z. Lin and Q. Ling, *J. Mater. Chem. C*, 2015, **3**, 7267–7271.
22 J. Ling, B. Daly, V. A. D. Silverson and A. P. de Silva, *Chem. Commun.*, 2015, **51**, 8403–8409.
23 W.-L. Gong, M. P. Aldred, G.-F. Zhang, C. Li and M.-Q. Zhu, *J. Mater. Chem. C*, 2013, **1**, 7519.
24 X. He, Z. Li, M. Chen and N. Ma, *Angew. Chem., Int. Ed.*, 2014, **126**, 14675–14678.
25 X. J. Jiang and D. K. Ng, *Angew. Chem., Int. Ed.*, 2014, **53**, 10481–10484.
26 M. Kumar, N. Kumar and V. Bhalla, *Chem. Commun.*, 2013, **49**, 877–879.
27 Y. Zhai, Z. Zhu, C. Zhu, J. Zhu, J. Ren, E. Wang and S. Dong, *Nanoscale*, 2013, **5**, 4344–4350.
28 D. Kim and T. S. Lee, *Chem. Commun.*, 2014, **50**, 5833–5836.
29 R. Orbach, F. Remacle, R. D. Levine and I. Willner, *Chem. Sci.*, 2014, **5**, 1074–1081.
30 D. Tong, H. Duan, J. Wang, Z. Yang and Y. Lin, *Sens. Actuators, B*, 2014, **195**, 80–84.
31 P. Remón, R. Ferreira, J.-M. Montenegro, R. Suau, E. Pérez-Inestrosa and U. Pischel, *ChemPhysChem*, 2009, **10**, 2004–2007.
32 A. K. Singh, P. K. Yadav, N. Kumari, R. Nagarajan and L. Mishra, *J. Mater. Chem. C*, 2015, **3**, 12123–12129.
33 M. Li, Z. Guo, W. Zhu, F. Marken and T. D. James, *Chem. Commun.*, 2015, **51**, 1293–1296.
34 P. Singh, H. Singh, G. Bhargava and S. Kumar, *J. Mater. Chem. C*, 2015, **3**, 5524–5532.
35 Z. Lin, Y.-D. Lin, C.-Y. Wu, P.-T. Chow, C.-H. g. Sun and T. Chow, *Macromolecules*, 2010, **43**, 5925–5931.
36 Y.-S. Lee, Z. Lin, Y.-Y. Chen, C.-Y. Liu and T. J. Chow, *Org. Electron.*, 2010, **11**, 604–612.
37 Z. Lin, Y.-S. Wen and T. Chow, *J. Mater. Chem.*, 2009, **19**, 5141–5148.
38 T.-S. Yeh, T. J. Chow, S.-H. Tsai, C.-W. Chiu and C.-X. Zhao, *Chem. Mater.*, 2006, **18**, 832–839.
39 Z. Lin, Y. Ma, X. Zheng, L. Huang, E. Yang, C.-Y. Wu, T. J. Chow and Q. Ling, *Dyes Pigm.*, 2015, **113**, 129–137.
40 Z. Lin, H. C. Chen, S.-S. Sun, C.-P. Hsu and T. J. Chow, *Tetrahedron*, 2009, **65**, 5216–5221.
41 N. Sarkar, K. Das, D. N. Nath and K. Bhattacharyya, *Langmuir*, 1994, **10**, 326–329.
42 M. M. Faul, K. A. Sullivan and L. L. Winneroski, *Synthesis*, 1995, **12**, 1511–1516.

43 B. K. Kaletaş, C. Mandl, G. van der Zwan, M. Fanti, F. Zerbetto, L. De Cola, B. König and R. M. Williams, *J. Phys. Chem. A*, 2005, **109**, 6440–6449.
44 K. Saita, M. Nakazono, K. Zaitsu, S. Nanbu and H. Sekiya, *J. Phys. Chem. A*, 2009, **113**, 8213–8220.
45 D. Aldakov and J. P. Anzenbacher, *Chem. Commun.*, 2003, 1394–1395.
46 P. Anzenbacher Jr, K. Jursikova, D. Aldakov, M. Marquez and R. Pohl, *Tetrahedron*, 2004, **60**, 11163–11168.